

Fundamentals of the Discrete Haar Wavelet Transform

Duraisamy Sundararajan

Abstract—The discrete wavelet transform, a generalization of the Fourier analysis, is widely used in several signal and image processing applications. In this paper, the fundamentals of the discrete Haar wavelet transform are presented from signal processing and Fourier analysis point of view. Fast algorithms for the implementation of Haar discrete wavelet transform, for both 1-D and 2-D signals, are presented.

1 Introduction

Fourier analysis is the approximation of an arbitrary signal by a sum of sinusoidal waveforms. Therefore, the study of the Fourier analysis begins with the study of the sinusoidal waveforms. The sinusoids used in the Fourier analysis have constant amplitude and are referred as constant-amplitude sinusoids. Expressing an arbitrary signal in terms of constant-amplitude sinusoids provides efficient methods to solve many practical problems. However, exponentially unbounded signals cannot be expressed in terms of constant-amplitude sinusoids. To analyze this class of signals, the Fourier analysis is generalized by including varying-amplitude sinusoids in the set of basis functions. This generalization is the Laplace transform for continuous signals and the z -transform for discrete signals. It is well-known that Fourier analysis is used for steady-state and spectral analysis while the Laplace and z -transforms are used for the design, transient, and stability analysis of systems. The point is that transformation of a signal (changing the form) is the fundamental method for efficient signal and system analysis. Several transforms are used in signal and system analysis and each transform is more suitable for some applications. As signals mostly occur in the time-domain, they have to be transformed to the other domain, processed, and transformed back to the time-domain. Therefore, for each transform, there exists forward and inverse versions.

2 The 1-D Discrete Haar Wavelet Transform

While a signal has to be decomposed in terms of its constituent individual sinusoids (Fourier analysis) for spectral analysis and fast evaluation of the convolution operation, it is found that the decomposition of a signal in terms of its components corresponding to different bands of the frequency spectrum (wavelet transform analysis) is suitable for applications such as signal compression, with reduced computational complexity of $O(N)$ rather than $O(N \log_2 N)$. The discrete version of this transform, which is similar to the discrete Fourier transform (DFT), is called the discrete wavelet transform (DWT). The DWT can be interpreted as spectral analysis using a set of basis functions those are localized in both time and frequency, in contrast to the infinite-extent sinusoids used in Fourier analysis. Unlike in the case of the DFT, there are several sets of basis functions used in the DWT. In this paper, we use the Haar basis functions only. These functions are the oldest [1] and the simplest of all the practically used DWT basis functions. Although it is the simplest, it is useful in DWT applications. In addition, it is the best version to understand the basic concepts of the DWT. The 2-point single-scale DWT of

the time-domain signal $\{x(0), x(1)\}$ and its inverse DWT (IDWT) are defined as

$$\begin{bmatrix} X_\phi(0,0) \\ X_\psi(0,0) \end{bmatrix} = \begin{bmatrix} \frac{1}{\sqrt{2}} & \frac{1}{\sqrt{2}} \\ \frac{1}{\sqrt{2}} & -\frac{1}{\sqrt{2}} \end{bmatrix} \begin{bmatrix} x(0) \\ x(1) \end{bmatrix} \quad \text{or} \quad \mathbf{X} = \mathbf{H}_{2,0}\mathbf{x} \quad \text{and} \quad \mathbf{x} = \mathbf{H}_{2,0}^{-1}\mathbf{X} = \mathbf{H}_{2,0}^T\mathbf{X}, \quad (1)$$

where \mathbf{X} , $\mathbf{H}_{2,0}$, and, \mathbf{x} represent, respectively, the coefficient, transform, and input matrices. As in the case of the FFT algorithms, it is assumed that the length N of a sequence

$$\{x(0), x(1), x(2), \dots, x(N-1)\}$$

is a power of 2. There are $J = \log_2(N)$ scales,

$$j = 0, 1, 2, \dots, J-1,$$

of decomposition possible for a given N . The corresponding coefficients belong to different starting scales. For $N = 2$, there is only one possible scale, designated as $j_0 = 0$. The number of scales of decomposition is determined based on the application requirements. Single-scale decomposition produces two components of a signal. The decomposition of a signal by n scales produces $n+1$ components of a signal. The 8-point single-scale DWT with starting scale $j_0 = 2$ of the time-domain signal

$$\{x(0), x(1), x(2), x(3), x(4), x(5), x(6), x(7)\}$$

is defined as

$$\begin{bmatrix} X_\phi(2,0) \\ X_\phi(2,1) \\ X_\phi(2,2) \\ X_\phi(2,3) \\ X_\psi(2,0) \\ X_\psi(2,1) \\ X_\psi(2,2) \\ X_\psi(2,3) \end{bmatrix} = \begin{bmatrix} \frac{1}{\sqrt{2}} & \frac{1}{\sqrt{2}} & 0 & 0 & 0 & 0 & 0 & 0 \\ 0 & 0 & \frac{1}{\sqrt{2}} & \frac{1}{\sqrt{2}} & 0 & 0 & 0 & 0 \\ 0 & 0 & 0 & 0 & \frac{1}{\sqrt{2}} & \frac{1}{\sqrt{2}} & 0 & 0 \\ 0 & 0 & 0 & 0 & 0 & 0 & \frac{1}{\sqrt{2}} & \frac{1}{\sqrt{2}} \\ \frac{1}{\sqrt{2}} & -\frac{1}{\sqrt{2}} & 0 & 0 & 0 & 0 & 0 & 0 \\ 0 & 0 & \frac{1}{\sqrt{2}} & -\frac{1}{\sqrt{2}} & 0 & 0 & 0 & 0 \\ 0 & 0 & 0 & 0 & \frac{1}{\sqrt{2}} & -\frac{1}{\sqrt{2}} & 0 & 0 \\ 0 & 0 & 0 & 0 & 0 & 0 & \frac{1}{\sqrt{2}} & -\frac{1}{\sqrt{2}} \end{bmatrix} \begin{bmatrix} x(0) \\ x(1) \\ x(2) \\ x(3) \\ x(4) \\ x(5) \\ x(6) \\ x(7) \end{bmatrix} \quad (2)$$

In the DWT, the transformed domain is the time-scale domain and the transformed values have time and scale as independent variables. Scale indicates the frequency band of the corresponding signal component. A higher scale number corresponds to a longer frequency band. The DWT coefficients are designated as $X_\phi(j_0, k)$ or $X_\psi(j, k)$. With a chosen $j = j_0$, $X_\phi(j_0, k)$ indicates the coefficients corresponding to the low frequency component called the approximation of the signal $x(n)$. Therefore, DWT coefficients $X_\phi(j_0, k)$ are called the approximation or scaling coefficients. The value $j_0 = 0$ indicates that the signal has been decomposed by the maximum of J scales. With $j_0 \leq j \leq J-1$, $X_\psi(j, k)$ indicates the coefficients corresponding to the high frequency components called the detail parts. Therefore, DWT coefficients $X_\psi(j, k)$ are called the detail or wavelet coefficients. The range of the index k (represents time position) is

$$k = 0, 1, 2, \dots, 2^j - 1$$

Given signal $x(n)$ is the same as $X_\phi(J, k)$. The highest scale scaling coefficients are the samples of the signal itself. While the 2-point DWT definition is the same as that of the 2-point DFT except for the constant factor, for longer sequence lengths N , the single-scale DWT is essentially

a set of $N/2$ 2-point DFTs of adjacent pairs of the input sequence. As the DWT is a generalized version of the Fourier analysis (a combination of a set of sinusoids belonging to a frequency group constitutes a component rather than the individual sinusoids as in Fourier analysis), adding a higher scale component to the approximation yields a partially reconstructed signal that is closer to the given signal. The number of higher scale detail or wavelet components used is determined by the application requirements.

The inverse transform matrix is the transpose of the forward transform matrix. These matrices are orthonormal and their product is an identity matrix. The 8-point single-scale IDWT (a set of four 2-point IDFTs) of the time-scale domain sequence

$$\{X_\phi(2,0), X_\phi(2,1), X_\phi(2,2), X_\phi(2,3), X_\psi(2,0), X_\psi(2,1), X_\psi(2,2), X_\psi(2,3)\}$$

is defined as

$$\begin{bmatrix} x(0) \\ x(1) \\ x(2) \\ x(3) \\ x(4) \\ x(5) \\ x(6) \\ x(7) \end{bmatrix} = \begin{bmatrix} \frac{1}{\sqrt{2}} & 0 & 0 & 0 & \frac{1}{\sqrt{2}} & 0 & 0 & 0 \\ \frac{1}{\sqrt{2}} & 0 & 0 & 0 & -\frac{1}{\sqrt{2}} & 0 & 0 & 0 \\ 0 & \frac{1}{\sqrt{2}} & 0 & 0 & 0 & \frac{1}{\sqrt{2}} & 0 & 0 \\ 0 & \frac{1}{\sqrt{2}} & 0 & 0 & 0 & -\frac{1}{\sqrt{2}} & 0 & 0 \\ 0 & 0 & \frac{1}{\sqrt{2}} & 0 & 0 & 0 & \frac{1}{\sqrt{2}} & 0 \\ 0 & 0 & \frac{1}{\sqrt{2}} & 0 & 0 & 0 & -\frac{1}{\sqrt{2}} & 0 \\ 0 & 0 & 0 & \frac{1}{\sqrt{2}} & 0 & 0 & 0 & \frac{1}{\sqrt{2}} \\ 0 & 0 & 0 & \frac{1}{\sqrt{2}} & 0 & 0 & 0 & -\frac{1}{\sqrt{2}} \end{bmatrix} \begin{bmatrix} X_\phi(2,0) \\ X_\phi(2,1) \\ X_\phi(2,2) \\ X_\phi(2,3) \\ X_\psi(2,0) \\ X_\psi(2,1) \\ X_\psi(2,2) \\ X_\psi(2,3) \end{bmatrix} \quad (3)$$

The transform matrix for single-scale DWT of a sequence of length N is given by

$$\mathbf{H}_{N,(\log_2(N)-1)} = \begin{bmatrix} \mathbf{I}_{\frac{N}{2}} \otimes \begin{bmatrix} \frac{1}{\sqrt{2}} & \frac{1}{\sqrt{2}} \\ \frac{1}{\sqrt{2}} & -\frac{1}{\sqrt{2}} \end{bmatrix} \\ \mathbf{I}_{\frac{N}{2}} \otimes \begin{bmatrix} \frac{1}{\sqrt{2}} & -\frac{1}{\sqrt{2}} \\ \frac{1}{\sqrt{2}} & \frac{1}{\sqrt{2}} \end{bmatrix} \end{bmatrix} \quad (4)$$

Note that $\mathbf{A} \otimes \mathbf{B} = [a_{ij}\mathbf{B}]$. The transform matrix in Eq. (2) is for an 8-point single-scale DWT. For other scales, Eq. (5) can be used.

$$\begin{aligned} \mathbf{H}_{N,(\log_2(N)-2)} &= \mathbf{H}_{\frac{N}{2},(\log_2(N)-2)} \mathbf{H}_{N,(\log_2(N)-1)} \\ \mathbf{H}_{N,(\log_2(N)-3)} &= \mathbf{H}_{\frac{N}{4},(\log_2(N)-3)} \mathbf{H}_{\frac{N}{2},(\log_2(N)-2)} \mathbf{H}_{N,(\log_2(N)-1)} \\ &\dots \\ \mathbf{H}_{N,0} &= \mathbf{H}_{2,0} \mathbf{H}_{4,1} \dots \mathbf{H}_{\frac{N}{2},(\log_2(N)-2)} \mathbf{H}_{N,(\log_2(N)-1)} \end{aligned} \quad (5)$$

The two-scale N -point DWT is obtained by taking the single-scale DWT of the lower-half of the N single-scale DWT coefficients, leaving the upper-half unchanged. This process continues until we take the single-scale DWT of the lowest pair of the DWT coefficients. For example,

$$\mathbf{H}_{4,0} = \mathbf{H}_{2,0} \mathbf{H}_{4,1} \quad (6)$$

$$\mathbf{H}_{8,1} = \mathbf{H}_{4,1} \mathbf{H}_{8,2} \quad (7)$$

$$\mathbf{H}_{8,0} = \mathbf{H}_{2,0} \mathbf{H}_{4,1} \mathbf{H}_{8,2} \quad (8)$$

$$\mathbf{H}_{4,0} = \begin{bmatrix} \phi_{0,0}(n) \\ \psi_{0,0}(n) \\ \psi_{1,0}(n) \\ \psi_{1,1}(n) \end{bmatrix} = \begin{bmatrix} \frac{1}{2} & \frac{1}{2} & \frac{1}{2} & \frac{1}{2} \\ \frac{1}{2} & -\frac{1}{2} & 0 & 0 \\ \frac{1}{\sqrt{2}} & -\frac{1}{\sqrt{2}} & 0 & 0 \\ 0 & 0 & \frac{1}{\sqrt{2}} & -\frac{1}{\sqrt{2}} \end{bmatrix} = \begin{bmatrix} \frac{1}{\sqrt{2}} & -\frac{1}{\sqrt{2}} \\ \frac{1}{\sqrt{2}} & -\frac{1}{\sqrt{2}} \end{bmatrix} \begin{bmatrix} \frac{1}{\sqrt{2}} & \frac{1}{\sqrt{2}} & 0 & 0 \\ 0 & 0 & \frac{1}{\sqrt{2}} & \frac{1}{\sqrt{2}} \\ \frac{1}{\sqrt{2}} & -\frac{1}{\sqrt{2}} & 0 & 0 \\ 0 & 0 & \frac{1}{\sqrt{2}} & -\frac{1}{\sqrt{2}} \end{bmatrix} = \mathbf{H}_{2,0} \mathbf{H}_{4,1}$$

This is a partial matrix factorization of the two-scale 4-point DWT transform matrix. The multiplication of the 2×2 matrix with the two top rows of the rightmost 4×4 matrix results in the leftmost 4×4 matrix. Similarly,

$$\mathbf{H}_{8,1} = \begin{bmatrix} \phi_{1,0}(n) \\ \phi_{1,1}(n) \\ \psi_{1,0}(n) \\ \psi_{1,1}(n) \\ \psi_{2,0}(n) \\ \psi_{2,1}(n) \\ \psi_{2,2}(n) \\ \psi_{2,3}(n) \end{bmatrix} = \begin{bmatrix} \frac{1}{\sqrt{4}} & \frac{1}{\sqrt{4}} & \frac{1}{\sqrt{4}} & \frac{1}{\sqrt{4}} & 0 & 0 & 0 & 0 \\ 0 & 0 & 0 & 0 & \frac{1}{\sqrt{4}} & \frac{1}{\sqrt{4}} & \frac{1}{\sqrt{4}} & \frac{1}{\sqrt{4}} \\ \frac{1}{\sqrt{4}} & \frac{1}{\sqrt{4}} & -\frac{1}{\sqrt{4}} & -\frac{1}{\sqrt{4}} & 0 & 0 & 0 & 0 \\ 0 & 0 & 0 & 0 & \frac{1}{\sqrt{4}} & \frac{1}{\sqrt{4}} & -\frac{1}{\sqrt{4}} & -\frac{1}{\sqrt{4}} \\ \frac{1}{\sqrt{2}} & -\frac{1}{\sqrt{2}} & 0 & 0 & 0 & 0 & 0 & 0 \\ 0 & 0 & \frac{1}{\sqrt{2}} & -\frac{1}{\sqrt{2}} & 0 & 0 & 0 & 0 \\ 0 & 0 & 0 & 0 & \frac{1}{\sqrt{2}} & -\frac{1}{\sqrt{2}} & 0 & 0 \\ 0 & 0 & 0 & 0 & 0 & 0 & \frac{1}{\sqrt{2}} & -\frac{1}{\sqrt{2}} \end{bmatrix}$$

$$\mathbf{H}_{8,0} = \begin{bmatrix} \phi_{0,0}(n) \\ \psi_{0,0}(n) \\ \psi_{1,0}(n) \\ \psi_{1,1}(n) \\ \psi_{2,0}(n) \\ \psi_{2,1}(n) \\ \psi_{2,2}(n) \\ \psi_{2,3}(n) \end{bmatrix} = \begin{bmatrix} \frac{1}{\sqrt{8}} & \frac{1}{\sqrt{8}} & \frac{1}{\sqrt{8}} & \frac{1}{\sqrt{8}} & -\frac{1}{\sqrt{8}} & \frac{1}{\sqrt{8}} & \frac{1}{\sqrt{8}} & \frac{1}{\sqrt{8}} \\ \frac{1}{\sqrt{8}} & \frac{1}{\sqrt{8}} & \frac{1}{\sqrt{8}} & \frac{1}{\sqrt{8}} & 0 & 0 & -\frac{1}{\sqrt{8}} & -\frac{1}{\sqrt{8}} \\ \frac{1}{\sqrt{4}} & \frac{1}{\sqrt{4}} & -\frac{1}{\sqrt{4}} & -\frac{1}{\sqrt{4}} & 0 & 0 & 0 & 0 \\ 0 & 0 & 0 & 0 & \frac{1}{\sqrt{4}} & \frac{1}{\sqrt{4}} & -\frac{1}{\sqrt{4}} & -\frac{1}{\sqrt{4}} \\ \frac{1}{\sqrt{2}} & -\frac{1}{\sqrt{2}} & 0 & 0 & 0 & 0 & 0 & 0 \\ 0 & 0 & \frac{1}{\sqrt{2}} & -\frac{1}{\sqrt{2}} & 0 & 0 & 0 & 0 \\ 0 & 0 & 0 & 0 & \frac{1}{\sqrt{2}} & -\frac{1}{\sqrt{2}} & 0 & 0 \\ 0 & 0 & 0 & 0 & 0 & 0 & \frac{1}{\sqrt{2}} & -\frac{1}{\sqrt{2}} \end{bmatrix}$$

The norm (the square root of the sum of the squares) of each row is one. The first row of the basis functions $\phi_{0,0}(n)$ is called the scaling function. It has the same nonzero value for all its samples. The rest of the rows $\psi_{j,k}(n)$ are called the wavelet functions. The second row is a square pulse with mean zero. The third row is a compressed (by a factor of 2) and scaled (by $\sqrt{2}$) version the second row. The fourth row is a shifted version of the third row. The last four rows are the compressed, shifted, and scaled versions of the third row. The shifting of a finite-extent basis function is one distinct feature of the DWT. This feature makes it possible for time-frequency analysis. For example, if the DWT coefficient $X_\psi(2, 3)$ of a signal corresponding to the last row of the basis function $\psi_{2,3}(n)$ is zero, it indicates that there is no component in the signal corresponding to the frequency band of the basis function during the last two samples. Another distinct feature is that the duration of the nonzero samples of the wavelet functions varies, giving the multiresolution characteristic.

Time-frequency resolutions of the DWT, with $N = 8$, is shown in Fig. 1. A better frequency resolution (a shorter frequency band) at low frequencies and vice versa is appropriate for signal analysis in several applications. Note that the Fourier transform provides no time resolution, as the time variable disappears in the transformation process. Each group of basis functions corresponds to a distinct band of the frequency spectrum of the signal with frequency varying from 0 to π radians. The combination of all the bands spans the complete spectrum of the signal. With 8 samples, the DWT can decompose a signal into a maximum of four components (three scales, $j = 0, 1, 2$) corresponding to spectral bands

$$(0 - \frac{\pi}{8}), (\frac{\pi}{8} - \frac{\pi}{4}), (\frac{\pi}{4} - \frac{\pi}{2}), \text{ and } (\frac{\pi}{2} - \pi) \text{ radians}$$

This decomposition corresponds to letting $j_0 = 0$. The DWT coefficients, shown in groups corresponding to the frequency bands, are

$$\{X_\phi(0, 0)\}, \{X_\psi(0, 0)\}, \{X_\psi(1, 0), X_\psi(1, 1)\}, \{X_\psi(2, 0), X_\psi(2, 1), X_\psi(2, 2), X_\psi(2, 3)\}$$

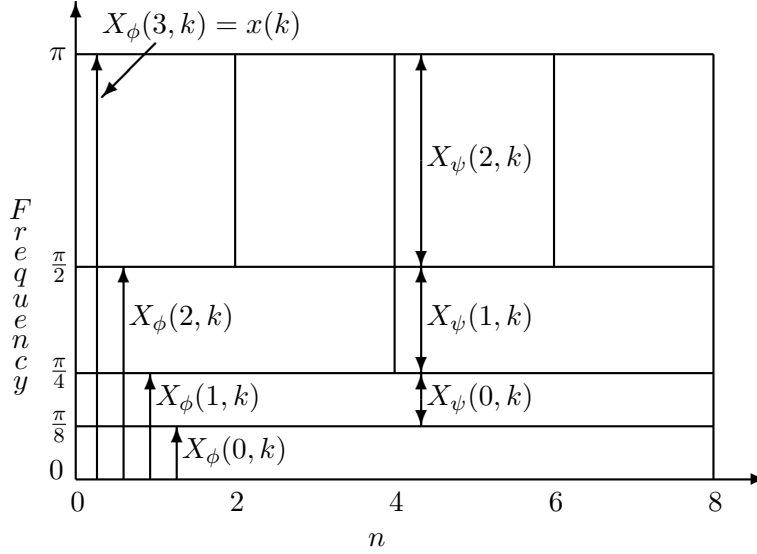


Figure 1: Time-frequency resolutions of the DWT, with $N = 8$

With $j_0 = 1$ (two scales, $j = 1, 2$), the spectral range is decomposed as

$$(0 - \frac{\pi}{4}), (\frac{\pi}{4} - \frac{\pi}{2}), \text{ and } (\frac{\pi}{2} - \pi) \text{ radians}$$

The corresponding DWT coefficients are

$$\{X_\phi(1, 0), X_\phi(1, 1)\}, \{X_\psi(1, 0), X_\psi(1, 1)\}, \{X_\psi(2, 0), X_\psi(2, 1), X_\psi(2, 2), X_\psi(2, 3)\}$$

With $j_0 = 2$, the spectral range is decomposed as

$$(0 - \frac{\pi}{2}) \text{ and } (\frac{\pi}{2} - \pi) \text{ radians}$$

The corresponding DWT coefficients are

$$\{X_\phi(2, 0), X_\phi(2, 1), X_\phi(2, 2), X_\phi(2, 3)\}, \{X_\psi(2, 0), X_\psi(2, 1), X_\psi(2, 2), X_\psi(2, 3)\}$$

With $j_0 = 3$, the spectral range is 0 to π radians. That is, the signal samples themselves are the approximation or scaling coefficients and no detail coefficients are required. All the decompositions are shown in Fig. 1. However, the decompositions, in practice, are not perfect. This is due to the fact that the frequency response of practical filters is not ideal. Fortunately, despite some errors in the decomposition, the original signal can be reconstructed exactly, as 2-point DFT is a reversible operation. The spectrum is divided equally on a logarithmic frequency scale, which resembles human perception.

Example

The DWT of

$$\{x(0) = 3, x(1) = 4, x(2) = 3, x(3) = -2\},$$

using $\mathbf{H}_{4,0}$ defined earlier, is given by

$$\begin{bmatrix} X_\phi(0, 0) \\ X_\psi(0, 0) \\ X_\psi(1, 0) \\ X_\psi(1, 1) \end{bmatrix} = \begin{bmatrix} \frac{1}{2} & \frac{1}{2} & \frac{1}{2} & \frac{1}{2} \\ \frac{1}{2} & \frac{1}{2} & -\frac{1}{2} & -\frac{1}{2} \\ \frac{1}{\sqrt{2}} & -\frac{1}{\sqrt{2}} & 0 & 0 \\ 0 & 0 & \frac{1}{\sqrt{2}} & -\frac{1}{\sqrt{2}} \end{bmatrix} \begin{bmatrix} 3 \\ 4 \\ 3 \\ -2 \end{bmatrix} = \begin{bmatrix} 4 \\ 3 \\ -\frac{1}{\sqrt{2}} \\ \frac{5}{\sqrt{2}} \end{bmatrix}$$

Each basis function contributes to the value of the time-domain waveform at each sample point. Therefore, multiplying each basis function by the corresponding DWT coefficient and summing the products gives the time-domain signal.

$$\begin{array}{cccccc} \left(\frac{1}{2} & \frac{1}{2} & \frac{1}{2} & \frac{1}{2}\right) & 4 & + \\ \left(\frac{1}{2} & \frac{1}{2} & -\frac{1}{2} & -\frac{1}{2}\right) & 3 & + \\ \left(\frac{1}{\sqrt{2}} & -\frac{1}{\sqrt{2}} & 0 & 0\right) & -\frac{1}{\sqrt{2}} & + \\ \left(0 & 0 & \frac{1}{\sqrt{2}} & -\frac{1}{\sqrt{2}}\right) & \frac{5}{\sqrt{2}} & = \\ \hline & 3 & 4 & 3 & -2 & \end{array}$$

Formally, the IDWT gets back the original input samples.

$$\begin{bmatrix} x(0) \\ x(1) \\ x(2) \\ x(3) \end{bmatrix} = \begin{bmatrix} \frac{1}{2} & \frac{1}{2} & \frac{1}{\sqrt{2}} & 0 \\ \frac{1}{2} & \frac{1}{2} & -\frac{1}{\sqrt{2}} & 0 \\ \frac{1}{2} & -\frac{1}{2} & 0 & \frac{1}{\sqrt{2}} \\ \frac{1}{2} & -\frac{1}{2} & 0 & -\frac{1}{\sqrt{2}} \end{bmatrix} \begin{bmatrix} 4 \\ 3 \\ -\frac{1}{\sqrt{2}} \\ \frac{5}{\sqrt{2}} \end{bmatrix} = \begin{bmatrix} 3 \\ 4 \\ 3 \\ -2 \end{bmatrix}$$

Note that the inverse transform matrix is the transpose of that of the forward transform matrix.

Parseval's theorem states that the sum of the squared-magnitude of a time-domain sequence equals the sum of the squared-magnitude of the corresponding transform coefficients. For the example sequence,

$$(3^2 + 4^2 + 3^2 + (-2)^2) = 38 = (4^2 + 3^2 + (-\frac{1}{\sqrt{2}})^2 + (\frac{5}{\sqrt{2}})^2)$$

3 The Fast Wavelet Transform

The fast wavelet transform (FWT), an algorithm for the fast computation of the Haar DWT, is just the implementation of Eq. (5). For example, the signal-flow graph of the 8-point three-scale FWT algorithm is shown in Fig. 2. The only difference is that the multiplications by the factor $1/\sqrt{2}$ are merged as much as possible. The partial values at various stages of the 8-point FWT algorithm are shown in Fig. 3. For the same input, single-scale DWT coefficients

$$\frac{1}{\sqrt{2}}\{1, 5, 9, 13, -1, -1, -1, -1\}$$

are obtained by multiplying the first-half values of the stage 1 output by $1/\sqrt{2}$. Two-scale DWT coefficients

$$\{3, 11, -2, -2, -\frac{1}{\sqrt{2}}, -\frac{1}{\sqrt{2}}, -\frac{1}{\sqrt{2}}, -\frac{1}{\sqrt{2}}\}$$

are obtained by multiplying the first-quarter values of the stage 2 output by $1/2$. For a N -point sequence, the number of real multiplications required for FWT is

$$\frac{N}{2} + \frac{N}{4} + \dots + 4 + 2 + 2 = N$$

The number of real additions required for FWT is

$$N + \frac{N}{2} + \dots + 4 + 2 = 2N - 2$$

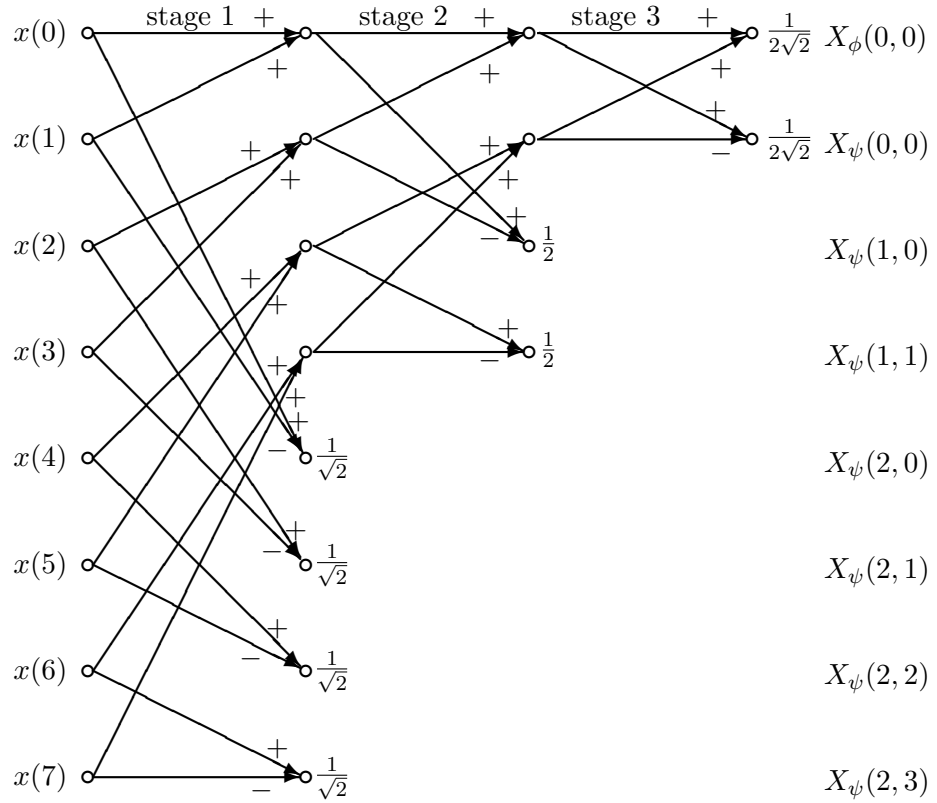


Figure 2: The signal-flow graph of the 1-D Haar three-scale FWT algorithm, with $N = 8$

	Input	Stage 1 Output	Stage 2 Output	Output
$x(0)$	0	1	6	$\frac{14}{\sqrt{2}} X_\phi(0,0)$
$x(1)$	1	5	22	$-\frac{8}{\sqrt{2}} X_\psi(0,0)$
$x(2)$	2	9	-2	$X_\psi(1,0)$
$x(3)$	3	13	-2	$X_\psi(1,1)$
$x(4)$	4	$-\frac{1}{\sqrt{2}}$		$X_\psi(2,0)$
$x(5)$	5	$-\frac{1}{\sqrt{2}}$		$X_\psi(2,1)$
$x(6)$	6	$-\frac{1}{\sqrt{2}}$		$X_\psi(2,2)$
$x(7)$	7	$-\frac{1}{\sqrt{2}}$		$X_\psi(2,3)$

Figure 3: The trace of the 1-D Haar three-scale FWT algorithm, with $N = 8$

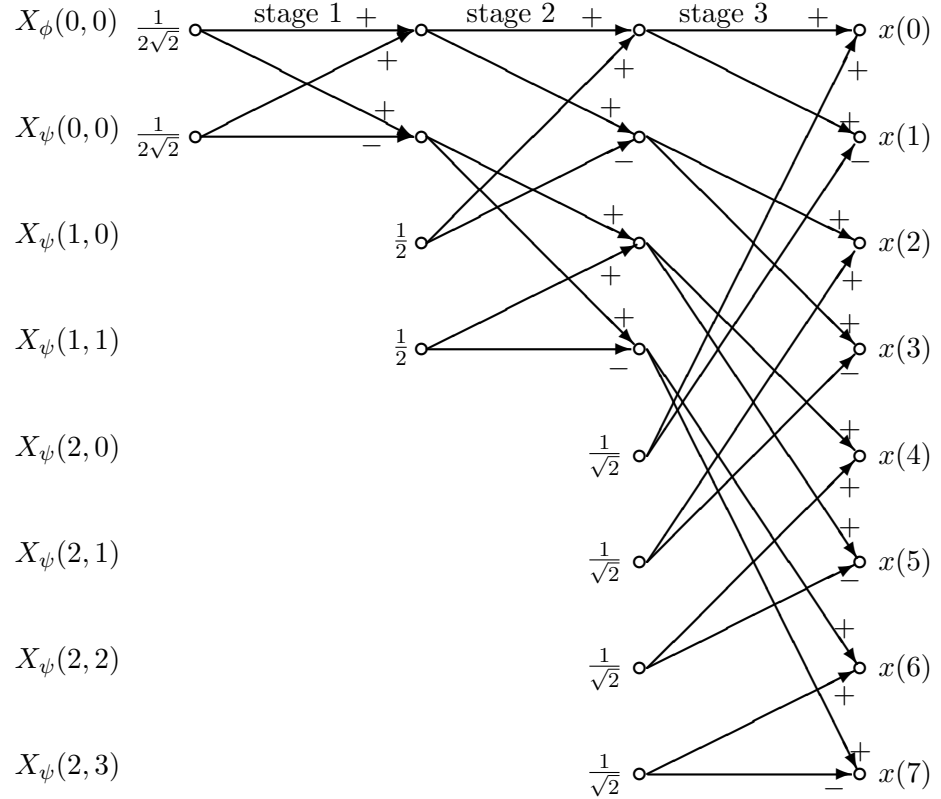


Figure 4: The signal-flow graph of the 1-D Haar three-scale IFFT algorithm, with $N = 8$

Therefore, the computational complexity of evaluating the Haar DWT using FFT is $O(N)$. The IFFT algorithm is obtained by partial factorization of the inverse transform matrix. For example, with $N = 4$,

$$\begin{bmatrix} \frac{1}{2} & \frac{1}{2} & \frac{1}{\sqrt{2}} & 0 \\ \frac{1}{2} & \frac{1}{2} & -\frac{1}{\sqrt{2}} & 0 \\ \frac{1}{2} & -\frac{1}{2} & 0 & \frac{1}{\sqrt{2}} \\ \frac{1}{2} & -\frac{1}{2} & 0 & -\frac{1}{\sqrt{2}} \end{bmatrix} = \begin{bmatrix} \frac{1}{\sqrt{2}} & 0 & \frac{1}{\sqrt{2}} & 0 \\ \frac{1}{\sqrt{2}} & 0 & -\frac{1}{\sqrt{2}} & 0 \\ 0 & \frac{1}{\sqrt{2}} & 0 & \frac{1}{\sqrt{2}} \\ 0 & \frac{1}{\sqrt{2}} & 0 & -\frac{1}{\sqrt{2}} \end{bmatrix} \begin{bmatrix} \frac{1}{\sqrt{2}} & \frac{1}{\sqrt{2}} \\ \frac{1}{\sqrt{2}} & -\frac{1}{\sqrt{2}} \end{bmatrix}$$

the multiplication of the two first two columns of the rightmost 4×4 matrix with the 2×2 matrix results in the leftmost 4×4 matrix, which is the two-scale 4-point inverse transform matrix.

The signal-flow graph of the 8-point three-scale IFFT algorithm is shown in Fig. 4. The partial values at various stages of the 8-point IFFT algorithm are shown in Fig. 5. The Matlab codes for these algorithms appear in the code snippet section of the dsprelated.com website.

4 Typical Applications

The 512 samples of an arbitrary signal is shown in Fig. 6(a). The spectrum of practical signals tends to fall off to insignificant levels at high frequencies. Therefore, the higher frequency components of a signal can be coded with less number of bits. The more compact the signal is coded (more efficiently compressed), the more is the reduction of storage and bandwidth

	Input	Stage 1 Output	Stage 2 Output	Output
$X_\phi(0,0)$	$\frac{14}{\sqrt{2}}$	$\frac{3}{2}$	$\frac{1}{2}$	0 $x(0)$
$X_\psi(0,0)$	$-\frac{8}{\sqrt{2}}$	$\frac{11}{2}$	$\frac{5}{2}$	1 $x(1)$
$X_\psi(1,0)$	-2		$\frac{9}{2}$	2 $x(2)$
$X_\psi(1,1)$	-2		$\frac{13}{2}$	3 $x(3)$
$X_\psi(2,0)$	$-\frac{1}{\sqrt{2}}$			4 $x(4)$
$X_\psi(2,1)$	$-\frac{1}{\sqrt{2}}$			5 $x(5)$
$X_\psi(2,2)$	$-\frac{1}{\sqrt{2}}$			6 $x(6)$
$X_\psi(2,3)$	$-\frac{1}{\sqrt{2}}$			7 $x(7)$

Figure 5: The trace of the 1-D Haar three-scale IFFT algorithm, with $N = 8$

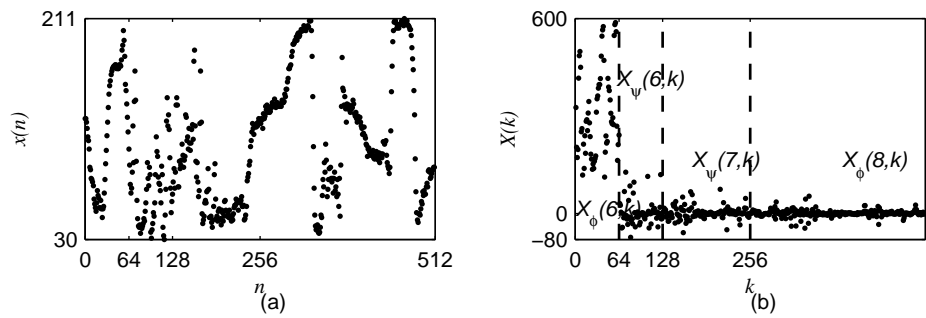


Figure 6: (a) An arbitrary signal; (b) The three-scale DWT decomposition of the signal

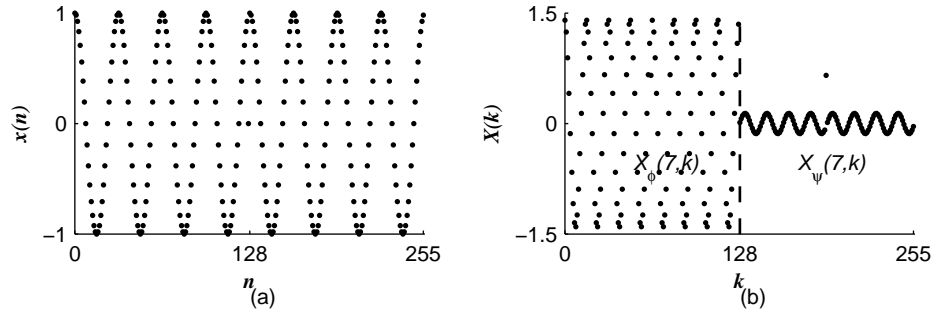


Figure 7: (a) A signal with a discontinuity; (b) The single-scale DWT decomposition of the signal showing the occurrence of the discontinuity

requirements. The three-scale DWT decomposition of the signal is shown in Fig. 6(b). The amplitude of the signal level, in each of the last three components, is much closer to zero than that of the preceding lower-frequency component.

In the DWT, the representation and analysis of signals are carried out at more than one resolution. Important features of a signal are likely to be detected at the least with one of the representations. Consider a sinusoidal signal with a discontinuity, as shown in Fig. 7(a). The time resolution of higher scale basis functions is better. Therefore, single-scale DWT decomposition of the signal, shown in Fig. 7(b), clearly shows the occurrence of the discontinuity in the detail component.

5 The 2-D Discrete Haar Wavelet Transform

The 2-D Haar DWT basis functions are separable. The 2-D DWT can be computed by the row-column method used for computing the 2-D DFT [2]. The 1-D FWT algorithm is used to compute the 1-D DWT of each column of the input data followed by computing the 1-D DWT of each row of the resulting data. Of course, the order of the computation can also be reversed.

In contrast to the computation of the 2-D DFT, single-scale DWT has to be used in a recursive manner to compute the 2-D DWT. Each decomposition of an image produces one approximation component $X_\phi(j, m, n)$ and three detail components, $X_\psi^H(j, m, n)$, $X_\psi^V(j, m, n)$, and $X_\psi^D(j, m, n)$. Component $X_\phi(j, m, n)$ is a smoothed version of the input. It almost resembles the original signal, since it is well known that the low-frequency part of the spectrum approximates a signal well. Components $X_\psi^H(j, m, n)$, $X_\psi^V(j, m, n)$, and $X_\psi^D(j, m, n)$ have high absolute values along vertical, horizontal and diagonal contours, respectively.

The DWT computation of the 2-D data \mathbf{x} and its inverse are defined as

$$\mathbf{X} = \mathbf{H}\mathbf{x}\mathbf{H}^T \quad \text{and} \quad \mathbf{x} = \mathbf{H}^T\mathbf{X}\mathbf{H}, \quad (9)$$

where \mathbf{H} is the appropriate 1-D Haar transform matrix. Postmultiplying the image matrix by the right transform matrix is computing 1-D DWT of the rows. Premultiplying the image matrix by the left transform matrix is computing 1-D DWT of the columns.

With the single-scale N-point 1-D transform matrix \mathbf{H} partitioned as

$$\mathbf{H} = \begin{bmatrix} [\mathbf{L}] \\ [\mathbf{H}] \end{bmatrix}, \quad \mathbf{H}\mathbf{x}\mathbf{H}^T = \begin{bmatrix} \mathbf{L} \\ \mathbf{H} \end{bmatrix} \mathbf{x} \begin{bmatrix} \mathbf{L} \\ \mathbf{H} \end{bmatrix}^T = \begin{bmatrix} \mathbf{L}\mathbf{x} \\ \mathbf{H}\mathbf{x} \end{bmatrix} \begin{bmatrix} \mathbf{L}^T & \mathbf{H}^T \end{bmatrix}$$

$$= \begin{bmatrix} \mathbf{LxL}^T & \mathbf{LxH}^T \\ \mathbf{HxL}^T & \mathbf{HxH}^T \end{bmatrix} = \begin{bmatrix} \mathbf{X}_\phi & \mathbf{X}_\psi^H \\ \mathbf{X}_\psi^V & \mathbf{X}_\psi^D \end{bmatrix} \quad (10)$$

In the following example, the 2-D DWT of a 2×2 data is computed by first computing the 1-D DWT of the columns followed by computing the 1-D DWT of the rows of the resulting data.

$$\begin{bmatrix} \frac{1}{\sqrt{2}} & \frac{1}{\sqrt{2}} \\ \frac{1}{\sqrt{2}} & -\frac{1}{\sqrt{2}} \end{bmatrix} \begin{bmatrix} 2 & 5 \\ 1 & 7 \end{bmatrix} \rightarrow \begin{bmatrix} \frac{3}{\sqrt{2}} & \frac{12}{\sqrt{2}} \\ \frac{1}{\sqrt{2}} & -\frac{2}{\sqrt{2}} \end{bmatrix} \begin{bmatrix} \frac{1}{\sqrt{2}} & \frac{1}{\sqrt{2}} \\ \frac{1}{\sqrt{2}} & -\frac{1}{\sqrt{2}} \end{bmatrix} = \begin{bmatrix} \frac{15}{2} & -\frac{9}{2} \\ -\frac{1}{2} & \frac{3}{2} \end{bmatrix}$$

Now, the same 2-D DWT is computed by first computing the 1-D DWT of the rows followed by computing the 1-D DWT of the columns of the resulting data.

$$\begin{bmatrix} 2 & 5 \\ 1 & 7 \end{bmatrix} \begin{bmatrix} \frac{1}{\sqrt{2}} & \frac{1}{\sqrt{2}} \\ \frac{1}{\sqrt{2}} & -\frac{1}{\sqrt{2}} \end{bmatrix} \rightarrow \begin{bmatrix} \frac{1}{\sqrt{2}} & \frac{1}{\sqrt{2}} \\ \frac{1}{\sqrt{2}} & -\frac{1}{\sqrt{2}} \end{bmatrix} \begin{bmatrix} \frac{7}{\sqrt{2}} & -\frac{3}{\sqrt{2}} \\ \frac{8}{\sqrt{2}} & -\frac{6}{\sqrt{2}} \end{bmatrix} = \begin{bmatrix} \frac{15}{2} & -\frac{9}{2} \\ -\frac{1}{2} & \frac{3}{2} \end{bmatrix}$$

The same computation is made using Eq. (10) yielding the same result.

$$\begin{aligned} \begin{bmatrix} \mathbf{LxL}^T & \mathbf{LxH}^T \\ \mathbf{HxL}^T & \mathbf{HxH}^T \end{bmatrix} &= \begin{bmatrix} \begin{bmatrix} \frac{1}{\sqrt{2}} & \frac{1}{\sqrt{2}} \end{bmatrix} \begin{bmatrix} 2 & 5 \\ 1 & 7 \end{bmatrix} \begin{bmatrix} \frac{1}{\sqrt{2}} \\ \frac{1}{\sqrt{2}} \end{bmatrix} & \begin{bmatrix} \frac{1}{\sqrt{2}} & \frac{1}{\sqrt{2}} \end{bmatrix} \begin{bmatrix} 2 & 5 \\ 1 & 7 \end{bmatrix} \begin{bmatrix} -\frac{1}{\sqrt{2}} \\ \frac{1}{\sqrt{2}} \end{bmatrix} \\ \begin{bmatrix} \frac{1}{\sqrt{2}} & -\frac{1}{\sqrt{2}} \end{bmatrix} \begin{bmatrix} 2 & 5 \\ 1 & 7 \end{bmatrix} \begin{bmatrix} \frac{1}{\sqrt{2}} \\ \frac{1}{\sqrt{2}} \end{bmatrix} & \begin{bmatrix} \frac{1}{\sqrt{2}} & -\frac{1}{\sqrt{2}} \end{bmatrix} \begin{bmatrix} 2 & 5 \\ 1 & 7 \end{bmatrix} \begin{bmatrix} -\frac{1}{\sqrt{2}} \\ \frac{1}{\sqrt{2}} \end{bmatrix} \end{bmatrix} \\ &= \begin{bmatrix} \frac{15}{2} & -\frac{9}{2} \\ -\frac{1}{2} & \frac{3}{2} \end{bmatrix} = \begin{bmatrix} \mathbf{X}_\phi & \mathbf{X}_\psi^H \\ \mathbf{X}_\psi^V & \mathbf{X}_\psi^D \end{bmatrix} \end{aligned}$$

Example

Consider computing the 2-D DWT of the following 4×4 2-D data.

$$x(n_1, n_2) = \begin{matrix} & n_2 \rightarrow \\ & \downarrow \\ n_1 & \begin{bmatrix} 1 & 2 & -1 & 3 \\ 2 & 1 & 4 & 3 \\ 1 & 1 & 2 & 2 \\ 4 & 2 & 1 & 3 \end{bmatrix} \end{matrix}$$

Computing the 1-D DWT of the rows of $x(n_1, n_2)$, we get

$$\begin{bmatrix} 2.1213 & 1.4142 & -0.7071 & -2.8284 \\ 2.1213 & 4.9497 & 0.7071 & 0.7071 \\ 1.4142 & 2.8284 & 0 & 0 \\ 4.2426 & 2.8284 & 1.4142 & -1.4142 \end{bmatrix}$$

Computing the 1-D DWT of the columns of the partially transformed matrix, we get the single-scale 2-D DWT of $x(n_1, n_2)$, shown in Fig. 8(a). Single-scale decomposition produces four components of a 2-D signal. The decomposition of a 2-D signal by n scales produces $3n+1$ components of the signal.

Computing the 1-D IDWT of the rows of the DWT coefficients shown in Fig. 8(a), we get

$$\begin{bmatrix} 2.1213 & 2.1213 & 2.1213 & 4.2426 \\ 3.5355 & 2.1213 & 2.1213 & 3.5355 \\ -0.7071 & 0.7071 & -3.5355 & 0 \\ -2.1213 & -0.7071 & 0.7071 & -0.7071 \end{bmatrix}$$

$$\begin{array}{c}
\begin{array}{cc|cc}
X_\phi(1, n_1, n_2) & X_\psi^H(1, n_1, n_2) & & \\
\hline
3 & 4.5 & 0 & -1.5 \\
4 & 4 & 1 & -1 \\
\hline
0 & -2.5 & -1 & -2.5 \\
-2 & 0 & -1 & 1 \\
\hline
X_\psi^V(1, n_1, n_2) & X_\psi^D(1, n_1, n_2) & &
\end{array} &
\begin{array}{c}
X_\psi^H(0, 0, 1) \\
\downarrow \\
X_\phi(0, 0, 0) \quad \downarrow \quad X_\psi^H(1, n_1, n_2) \\
\begin{array}{cc|cc}
\hline
7.75 & -0.75 & 0 & -1.5 \\
-0.25 & -0.75 & 1 & -1 \\
\hline
0 & -2.5 & -1 & -2.5 \\
-2 & 0 & -1 & 1 \\
\hline
X_\psi^V(1, n_1, n_2) & X_\psi^D(1, n_1, n_2) & & \\
\hline
X_\psi^D(0, 1, 1)
\end{array}
\end{array} \\
\begin{array}{c}
\text{(a)} \\
\text{(b)}
\end{array}
\end{array}$$

Figure 8: The single-scale and two-scale 2-D Haar DWT of $x(n_1, n_2)$

Note that the inverse transform matrix is the transpose of that of the forward transform matrix. Computing the 1-D IDWT of the columns of the partially transformed matrix, we get back $x(n_1, n_2)$.

Computing the 1-D row DWT of the 2×2 DWT coefficients shown at the top-left corner in Fig. 8(a), we get

$$\begin{bmatrix}
5.3033 & -1.0607 & 0 & -1.5 \\
5.6569 & 0 & 1 & -1 \\
0 & -2.5 & -1 & -2.5 \\
-2 & 0 & -1 & 1
\end{bmatrix}$$

Computing the 1-D column DWT of the top-left corner of the partially transformed matrix, we get the two-scale 2-D DWT of $x(n_1, n_2)$, shown in Fig. 8(b).

Computing the 1-D row IDWT of the 2×2 DWT coefficients shown at the top-left corner in Fig. 8(b), we get

$$\begin{bmatrix}
4.9497 & 6.0104 & 0 & -1.5 \\
-0.7071 & 0.3536 & 1 & -1 \\
0 & -2.5 & -1 & -2.5 \\
-2 & 0 & -1 & 1
\end{bmatrix}$$

Computing the 1-D column IDWT of the top-left corner of the partially transformed matrix, we get the single-scale DWT of $x(n_1, n_2)$ shown in Fig. 8(a). A single-scale 2-D IDWT will get back $x(n_1, n_2)$, as shown earlier. Examples of typical images decomposed to various scales can be found in [3].

6 Multirate digital signal processing and the DWT

The wavelet transform is essentially a set of bandpass filters and their efficient implementation. Because the 2-point Haar DWT is basically a 2-point DFT, the FWT is very similar to FFT. However, several other sets of basis functions are also used in DWT [4]. The study of the DWT using these basis functions is facilitated by the multirate digital signal processing theory. For each application of the DWT, a certain set of basis functions is more suitable.

Computation of the DWT using the convolution operation

The basic operation in finding the transform of a signal is the determination of its correlation with each of the basis functions. For example, the determination of the Fourier series is finding

the amplitudes of each of an infinite number of sinusoids by correlating the given waveform with each of its constituent sinusoids. While the functions of correlation and convolution are different, their computation is very similar. Carrying out the convolution operation without time-reversing either of the two functions is the correlation operation. The DFT operation is similar to that of a set of bandpass filters with a narrow passband. While individual sinusoids are filtered out in the DFT operation, the components of a signal corresponding to a set of bands of the frequency spectrum are filtered out in the DWT. The required operation is the convolution of the signal with the impulse responses of the corresponding filters. The impulse responses can be derived from the time-reversals of the 2-point Haar ($\mathbf{H}_{2,0}$) basis functions. As the decomposed signal components consist of a smaller number of sinusoids, each signal component is represented by a reduced set of samples. Reducing the number of samples is called the downsampling operation (discarding every other sample). After processing the individual components of a signal, the complete processed signal has to be reconstructed. The reconstruction process involves upsampling (inserting a zero after every sample) and filtering operations. Further, all these operations have to be carried out using efficient algorithms. Therefore, signal decomposition, downsampling, upsampling, and reconstruction constitute the essential multirate digital signal processing operations required for the implementation of the DWT.

The linear convolution of sequences $x(n)$ and $h(n)$ is given as

$$y(n) = \sum_{m=-\infty}^{\infty} x(m)h(n-m)$$

In the DWT decomposition of a signal, convolution (filtering) is followed by downsampling defined by

$$\begin{aligned} y_{\phi}(n) &= \sum_{m=2n}^{2n+1} x(m)h_{\phi}((2n+1)-m), \quad n = 0, 1, \dots, \frac{N}{2} - 1 \\ y_{\psi}(n) &= \sum_{m=2n}^{2n+1} x(m)h_{\psi}((2n+1)-m), \quad n = 0, 1, \dots, \frac{N}{2} - 1 \end{aligned}$$

In the DWT reconstruction of a signal, upsampling is followed by convolution (filtering) defined by

$$x(n) = \sum_{m=n-1}^n y_{\phi}^i(m)h_{\phi}(n-m) + \sum_{m=n-1}^n y_{\psi}^i(m)h_{\psi}(-(n-m)), \quad n = 0, 1, \dots, N-1$$

where $h_{\phi}(n) = \{1, 1\}$ and $h_{\psi}(n) = \{-1, 1\}$ and $y_{\phi}^i(m)$ and $y_{\psi}^i(m)$ are upsampled versions of $y_{\phi}(m)$ and $y_{\psi}(m)$. Note that the division by the constant $\sqrt{2}$ is not shown, for simplicity, in $h_{\phi}(n), h_{\psi}(n)$, Figs. 9, 10 and 11. The convolution of the input $\{x(0) = 3, x(1) = 4, x(2) = 3, x(3) = -2\}$ with the scaled impulse response $\{1, 1\}$ is shown in Fig. 9 on the left-hand side. The computation of single-scale Haar DWT approximation coefficients alone is shown on the right-hand side. The convolution of the input $\{x(0) = 3, x(1) = 4, x(2) = 3, x(3) = -2\}$ with the scaled impulse response $\{-1, 1\}$ is shown in Fig. 10 on the left-hand side. The computation of Haar DWT detail coefficients alone is shown on the right-hand side. The computation of Haar IDWT using the convolution operation is shown in Fig. 11. The DWT approximation coefficients $\{7, 1\}$ are upsampled to obtain $\{7, 0, 1, 0\}$ and convolved with the scaled impulse response $\{1, 1\}$ to get $\{7, 7, 1, 1, 0\}$. The DWT detail coefficients $\{-1, 5\}$ are

m	0	1	2	3	
$h_\phi(m)$	1	1			
$x(m)$	3	4	3	-2	
$h_\phi(0-m)$	1	1			
$h_\phi(1-m)$	1	1			
$h_\phi(2-m)$	1	1			
$h_\phi(3-m)$	1	1			
$h_\phi(4-m)$	1	1			
n	0	1	2	3	4
$y(n)$	3	7	7	1	-2

m	0	1	2	3	
$h_\phi(m)$	1	1			
$x(m)$	3	4	3	-2	
$h_\phi(1-m)$	1	1			
$h_\phi(3-m)$	1	1			
n	0				1
$y_\phi(n)$	7				1

Figure 9: The single-scale Haar DWT approximation coefficients using the convolution operation

m	0	1	2	3	
$h_\psi(m)$	-1	1			
$x(m)$	3	4	3	-2	
$h_\psi(0-m)$	1	-1			
$h_\psi(1-m)$	1	-1			
$h_\psi(2-m)$	1	-1			
$h_\psi(3-m)$	1	-1			
$h_\psi(4-m)$	1	-1			
n	0	1	2	3	4
$y(n)$	-3	-1	1	5	-2

m	0	1	2	3	
$h_\psi(m)$	-1	1			
$x(m)$	3	4	3	-2	
$h_\psi(1-m)$	1	-1			
$h_\psi(3-m)$	1	-1			
n	0				1
$y_\psi(n)$	-1				5

Figure 10: The single-scale Haar DWT detail coefficients using the convolution operation

m	0	1	2	3	
$h_\phi(m)$	1	1			
$y_\phi^i(m)$	7	0	1	0	
$h_\phi(0-m)$	1	1			
$h_\phi(1-m)$	1	1			
$h_\phi(2-m)$	1	1			
$h_\phi(3-m)$	1	1			
$h_\phi(4-m)$	1	1			
n	0	1	2	3	4
$x_{lp}(n)$	7	7	1	1	0

m	0	1	2	3	
$-h_\psi(m)$	1	-1			
$y_\psi^i(m)$	-1	0	5	0	
$-h_\psi(0-m)$	-1	1			
$-h_\psi(1-m)$	-1	1			
$-h_\psi(2-m)$	-1	1			
$-h_\psi(3-m)$	-1	1			
$-h_\psi(4-m)$	-1	1			
n	0	1	2	3	4
$x_{hp}(n)$	-1	1	5	-5	0

Figure 11: The single-scale Haar IDWT using the convolution operation

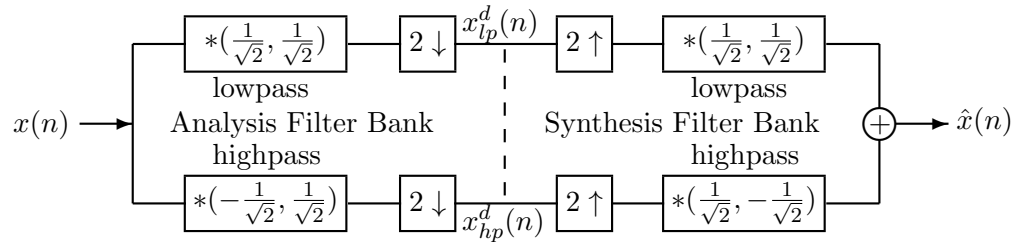


Figure 12: Quadrature mirror filter bank

upsampled to obtain $\{-1, 0, 5, 0\}$ and convolved with the scaled impulse response $\{1, -1\}$ to get $\{-1, 1, 5, -5, 0\}$. Note that these convolutions are just duplicating with and without sign change of each of the $N/2$ values to obtain N values. The first four samples of the summation of the two interpolated sequences

$$\{7, 7, 1, 1, 0\} + \{-1, 1, 5, -5, 0\} = \{6, 8, 6, -4, 0\}$$

are just two times that of the given input sequence $\{x(0) = 3, x(1) = 4, x(2) = 3, x(3) = -2\}$.

Quadrature mirror filter banks

Quadrature mirror filters are a pair of filters with frequency responses those are mirror images about the quadrature frequency $2\pi/4 = \pi/2$. Two such pairs constitute a two-channel quadrature mirror filter bank (QMF). The requirement for the four filters in the QMF, shown in Fig. 12, is that the output $\hat{x}(n)$ must be equal to the input if no processing of the subband components of the signal is made. Exact reconstruction is possible only with Haar filters, since the operations involved are 2-point DFT and 2-point IDFT. It is well-known that the IDFT of the DFT of a signal is the signal itself, that is the operations are reversible. The two filters in the upper channel are lowpass filters and the the other two filters are highpass filters. In the analysis section, downsampling operation is followed by the filtering operation. The filter, called antialiasing filter, is required to filter out the out of band frequencies for the particular filter to prevent aliasing. The output of the upper channel analysis filter bank is $x_{lp}^d(n)$, that is the decimated low-frequency or approximation component of the input sequence $x(n)$. The output of the other channel is $x_{hp}^d(n)$, that is the decimated high-frequency or detail component of $x(n)$. In the synthesis section, $x_{lp}^d(n)$ and $x_{hp}^d(n)$ are interpolated and then combined to reconstruct $x(n)$. In the reconstruction process, upsampling operation precedes the filtering operation. The filter, called anti-imaging filter, is required to filter out the image frequencies generated by the upsampling operation in each channel. The analysis (synthesis) section can be cascaded to compute the (IDWT) DWT with different number of input values and scales, as shown later.

It is obvious that interchanging the downsampler and the filter in the analysis section and interchanging the upsampler and the filter in the synthesis section will avoid unnecessary computations. It is through the use of polyphase decomposition and Noble identities, as shown in Fig. 13, the operation of the QMF becomes more efficient. The symbol z in the figure indicates that the signal is advanced by one sample interval. The symbol z^{-1} indicates that the signal is delayed by one sample interval.

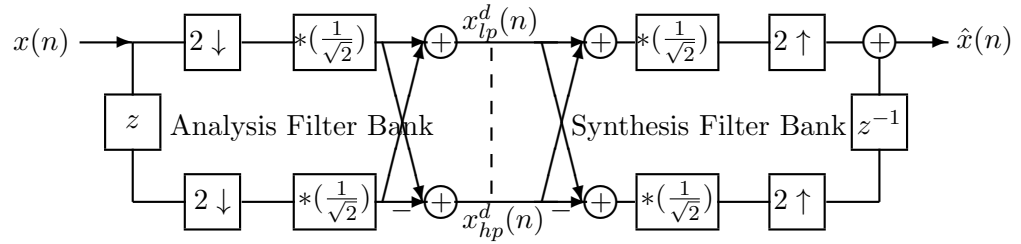


Figure 13: Efficient implementation of the QMF

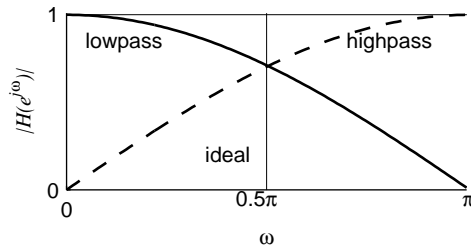


Figure 14: The magnitude of the frequency response of the Haar filters

Frequency response of the Haar filters

Consider a pair of samples $\{2, 3\}$ and its DFT $\{5, -1\}$. The signal is composed of two components, one with zero frequency and another with frequency π radians. In terms of its components,

$$\{2, 3\} = \left(\frac{5\{1, 1\} = \{5, 5\}}{2} \right) + \left(\frac{-1\{1, -1\} = \{-1, 1\}}{2} \right)$$

In the DFT interpretation, the pair of values $\{5, -1\}$ can be considered as the scaled coefficients of the two sinusoids, $\{1, 1\}$ and $\{1, -1\}$, constituting the signal $\{2, 3\}$. In the DWT interpretation, the pair of values $\{5, -1\}$ can be considered as the scaled first sample values of the low and high frequency components of the signal $\{2, 3\}$. Note that, as the frequency components are separated, one sample (from $\{5, 5\}$ and $\{-1, 1\}$) is sufficient to represent each of the components and they can be interpolated to get both the sample values. For a sequence length of two, the decomposition of the two components of the signal is perfect. With longer sequence lengths, the signal contains more frequency components. Correlation of the signal with shifted versions of $\{1, 1\}$ yields a smaller value with increasing frequencies. At the frequency π radians, the response is zero. The frequency response is one-quarter of a cosine wave, which is a lowpass filter (although not a good one). Correlation with the other basis function $\{1, -1\}$ yields a response that resembles a highpass filter. Let us derive the frequency responses of the Haar filters.

$$H_0(e^{j\omega}) = \frac{1}{\sqrt{2}}(1 + e^{j\omega}) = \frac{1}{\sqrt{2}}e^{j\frac{\omega}{2}}(e^{-j\frac{\omega}{2}} + e^{j\frac{\omega}{2}}) = \sqrt{2}e^{j\frac{\omega}{2}} \cos\left(\frac{\omega}{2}\right)$$

$$H_1(e^{j\omega}) = \frac{1}{\sqrt{2}}(1 - e^{j\omega}) = \frac{1}{\sqrt{2}}e^{j\frac{\omega}{2}}(e^{-j\frac{\omega}{2}} - e^{j\frac{\omega}{2}}) = -j\sqrt{2}e^{j\frac{\omega}{2}} \sin\left(\frac{\omega}{2}\right)$$

The magnitude of the frequency response of the Haar filters is shown in Fig. 14. The actual frequency responses are far from ideal. Therefore, some overlapping between frequency bands will occur. However, as only 2-point DFT and IDFT are involved, the result of taking DFT and IDFT gets back the original input values.

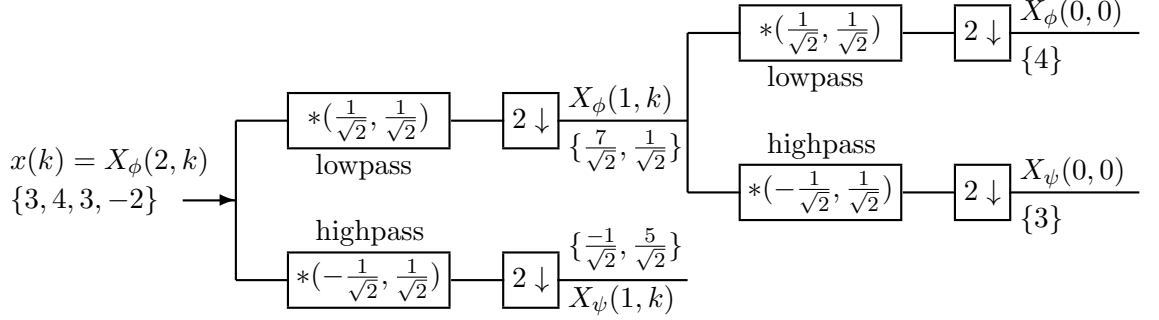


Figure 15: Computation of a two-scale 4-point DWT using a two-stage QMF bank

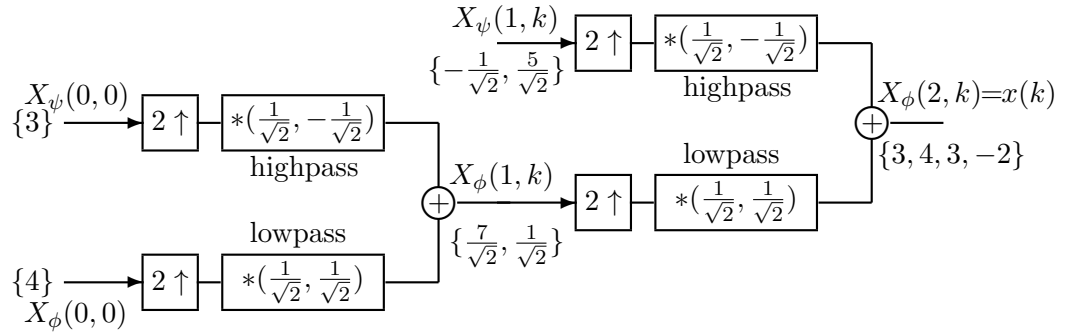


Figure 16: Computation of a two-scale 4-point IDWT using a two-stage QMF bank

Examples

Computation of a two-scale 4-point DWT using a two-stage QMF bank is shown in Fig. 15. Each filter bank decomposes a signal into two components without changing the data size. By cascading a number of QMFs, the required decomposition of a signal is obtained. Due to the downsampling operation by a factor of two, the sampling frequency gets divided by the same factor at every stage. Computation of a two-scale 4-point IDWT using a two-stage QMF bank is shown in Fig. 16.

Computation of a single-scale 4×4 2-D DWT using a two-stage QMF bank is shown in Fig. 17. Coefficients \mathbf{X}_ϕ are obtained by applying lowpass filtering and decimation to each row of the 2-D data \mathbf{x} followed by applying lowpass filtering and decimation to each column of the resulting data. Coefficients \mathbf{X}_ψ^H are obtained by applying highpass filtering and decimation to each row of the 2-D data \mathbf{x} followed by applying lowpass filtering and decimation to each column of the resulting data. Coefficients \mathbf{X}_ψ^V are obtained by applying lowpass filtering and decimation to each row of the 2-D data \mathbf{x} followed by applying highpass filtering and decimation to each column of the resulting data. Coefficients \mathbf{X}_ψ^D are obtained by applying highpass filtering and decimation to each row of the 2-D data \mathbf{x} followed by applying highpass filtering and decimation to each column of the resulting data. Computation of a single-scale 4×4 2-D IDWT using a two-stage QMF bank is shown in Fig. 18.

7 Summary

- Transformation (changing the form) of signals is essential for their efficient analysis and processing.

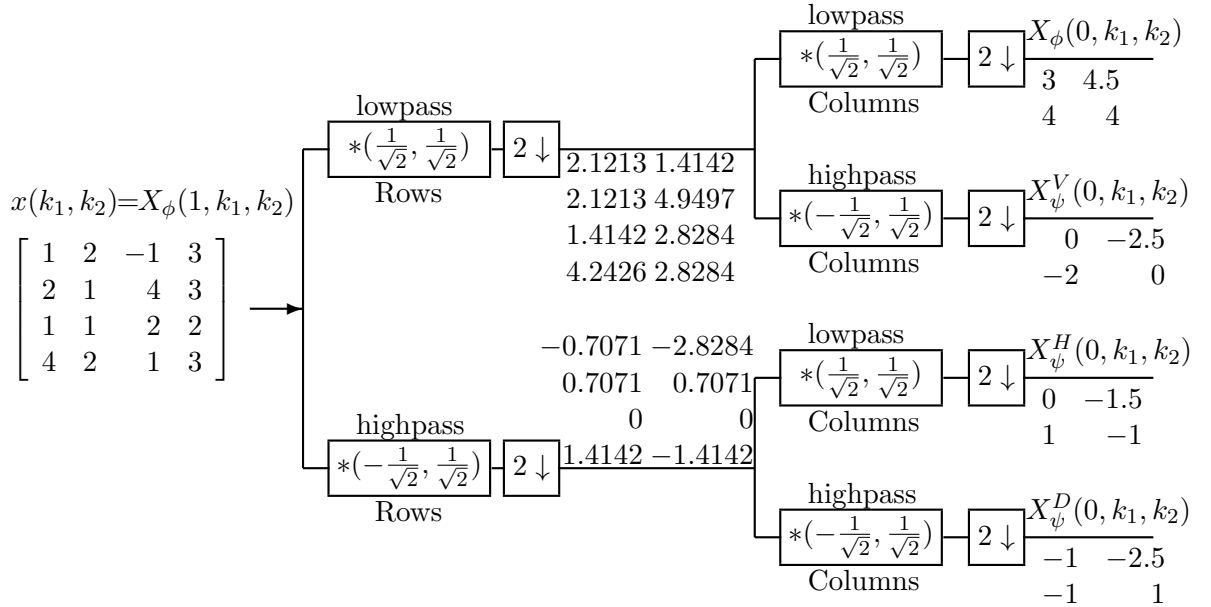


Figure 17: Computation of a single-scale 4×4 DWT using a two-stage QMF bank

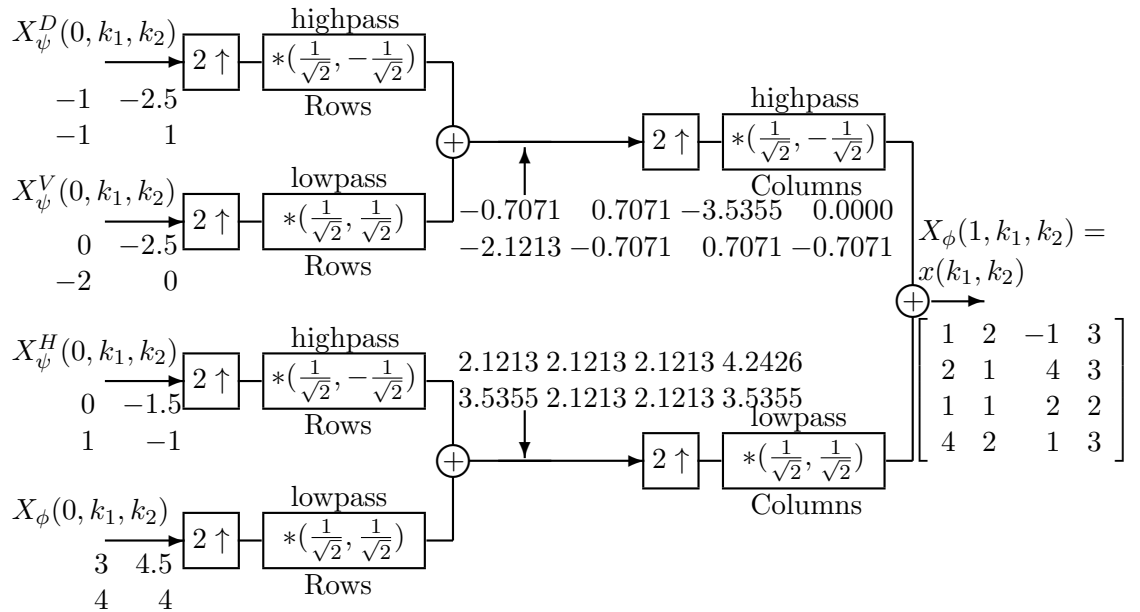


Figure 18: Computation of a single-scale 4×4 2-D IDWT using a two-stage QMF bank

- Fourier analysis decomposes a waveform in terms of signal components corresponding to individual sinusoids.
- The DWT decomposes a waveform in terms of signal components corresponding to different spectral bands, called subbands.
- The basis functions of the DWT are localized in both time and frequency.
- The DWT is essentially a set of bandpass filters.
- The DWT decomposition of a waveform and its reconstruction are carried out using a set of lowpass and highpass filters in a recursive and efficient manner.
- The computational complexity of computing the DWT is $O(N)$.
- The multiresolution capability of the DWT makes it possible to detect features at a resolution that may go undetected at another.
- The DWT is suitable for applications such as signal compression.

References

1. Haar, A. (1910). "Zur Theorie der Orthogonalen Funktionensysteme," *Math Annal.*, vol. 69, pp. 331-371.
2. Sundararajan, D. (2001) *Discrete Fourier Transform, Theory, Algorithms, and Applications*, World Scientific, Singapore.
3. Gonzalez, R. C. and Woods, R. E. (2008) *Digital Image Processing*, Prentice-Hall, New Jersey, U.S.A.
4. The Mathworks, (2011) *Matlab Wavelet Tool Box User's Guide*, The Mathworks, Inc. U.S.A.